ARTICLE NO. 79-4118

Geometric Analysis of Rosette® Exit Cones

N.J. Pagano*
Air Force Materials Laboratory, Wright-Patterson AFB, Ohio
and
P.W. Hsu†
University of Dayton Research Institute, Dayton, Ohio

An exploratory analysis of the geometry of Rosette® (registered trademark of Hitco) exit cones is carried out in the present work. The basic analysis begins with the premise that each horizontal cross section of the warped sheet (layer) follows a certain spiral trajectory governed by a set of equations which guarantee the continuity and axisymmetry requirements of the cone. While such a three-dimensional warped layer is not able to be developed from a flat basic sheet (e.g., a preimpregnated cloth material), a procedure based upon the preceding basic analysis is derived to construct the associated approximate flat sheet pattern. The errors associated with this procedure are calculated and found to be small for practical configurations, which indicates that the scheme is quite applicable in the actual fabrication of the rosette cone.

Introduction

EXTENSIVE use of rosette construction in rocket nozzles and exit cones has led to an exploratory analytical study[1] in which the potential of rosette construction to produce striking reductions in peak stress concentration compared to hoop-wound and helical-wound cylinders was demonstrated. It is now appropriate to extend the study of Ref. 1 to solve a related problem of practical interest, namely, the Rosette® cone. The type of rosette construction treated here is defined by generating spirals which lie in planes normal to the axis of the cone. In the present work, our attention shall be confined to the geometric aspects of the problem. This leads to the definition of the basic sheet configuration from which the cone is constructed. While the detailed motion of the sheets in a rosette body is quite complex, this motion is immaterial for the present purpose, which is to describe the initial sheet pattern leading to the *final* geometry, which in turn is defined by the sheet thickness in the final configuration. The analysis leading to the description of mechanical response will be presented in a subsequent report.

It may be recalled that the basic sheet pattern in Ref. 1 was rectangular. These fibrous sheets (or layers) can be distorted and placed, layer by layer, along certain spiral trajectories until a cylindrical body is formed. In such an exact development process, the flexible flat sheets are transformed into a three-dimensional body with identical horizontal cross sections. For a rosette cone, however, the three-dimensional body is generated by a warped surface, since its horizontal spiral cross section varies both in length and curvature with respect to the cone axis (Fig. 1). Since such a surface is not able to be developed,[2] it becomes necessary to formulate an approximate treatment so that the conical structure can be built from preimpregnated cloth. To this end, a numerical mapping process will be carried out to determine the approximate configuration, to assess the associated error, and to explore its sensitivity to the influence of the appropriate geometric parameters.

Basic Geometry

Consider the frustrum of a cone illustrated in Fig. 1. The body is to be generated from a set of identical warped sheets of uniform thickness. Each surface of a warped sheet originates on the outer periphery of the cone (such as points along AB) and terminates on the inner circumference, e.g., cuved line DC, or vice versa. Our present objective is to define the precise geometry of surface ABCD, which is consistent with the continuity requirement (complete filling of the volume with no gaps or overlaps). In the next section, the possibility of developing surface ABCD from a plane sheet shall be examined. The characteristic dimensions of the rosette cone are:

α_0 = arc angle at A, top point of a generator of the outer conical surface
R_0 = outer radius of top ring
R_I = inner radius of top ring
R_2 = inner radius of bottom ring
t = cone thickness
S = cone slant height along generator
β = cone half-angle
h = cone height

Guided by the results for the cylindrical case,[1] the analysis is begun by assuming that each warped sheet follows the trajectory

$$r \sin\alpha = c(z) \tag{1}$$

in every plane normal to the cone axis. Here c is a function of z alone. In Eq. (1), r is the radial distance in the cylindrical coordinate system and α is the local arc angle. Also, α_0 is independent of θ. In order to define the parameter $c(z)$, recall[1] that the number of layers N within a cylinder is given by

$$N = \frac{2\pi R_0 \sin\alpha_0}{t_I} = \frac{2\pi r \sin\alpha}{t_I} \tag{2}$$

where t_I is the thickness of a single layer measured in the plane z = const. Since N is a constant and t', the ply thickness, and t_I are approximately related by $t' = t_I \cos\beta$, a good first approximation is given by

$$c(z) = \text{const} \tag{3}$$

Received Sept. 7, 1978; revision received Jan. 12, 1979. This paper is declared a work of the U.S. Government and therefore is in the public domain. Reprints of this article may be ordered from AIAA Special Publications, 1290 Avenue of the Americas, New York, N.Y. 10019. Order by Article No. at top of page. Member price $2.00 each, nonmember, $3.00 each. **Remittance must accompany order.**

Index categories: Analytical and Numerical Methods; LV/M Structural Design (including Loads).

*Materials Research Engineer, Nonmetallic Materials Division.
†Assoc. Research Engineer, Nonmetallic Materials Division.
®Registered trademark of Hitco.

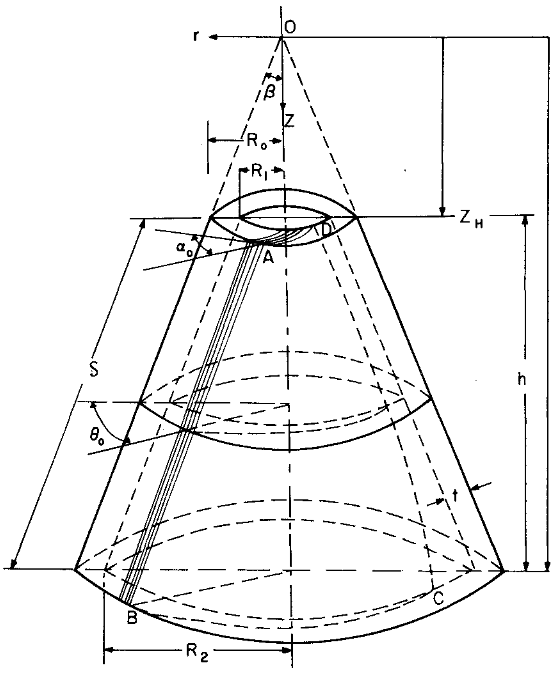

Fig. 1 Rosette cone geometry.

so that

$$r \sin\alpha = R_0 \sin\alpha_0 = \text{const} \tag{4}$$

for all values of z. Because of this approach to define the basic pattern, the structure becomes axisymmetric as in Ref. 1.

In Fig. 2, the top view of a typical cross section (z = const) shows the trace of a warped sheet which is a horizontal spiral. As in Ref. 1, these horizontal spirals satisfy the equation

$$\theta - \theta_0 = \bar{\alpha} + \cot\bar{\alpha} - \alpha - \cot\alpha \tag{5}$$

where, in the present case,

$$\bar{\alpha} = \sin^{-1}\left[\frac{R_0 \sin\alpha_0}{z \tan\beta}\right] \tag{6}$$

by Eq. (4). Here $\bar{\alpha}$ is the arc angle on the cone generator AB at a level z, i.e., points with coordinates ($z \tan\beta$, 0, z). For convenience, θ_0 is now set equal to zero. Thus, the generator AB becomes the reference line for θ. Then the arc length along each horizontal spiral takes the form

$$l = \frac{z^2\tan^2\beta - r^2}{2R_0\sin\alpha_0} \tag{7}$$

Since the wall thickness t is a constant (see Appendix for a cone of variable wall thickness), the total spiral length L can be determined as

$$L = k_1 z + k_2 \tag{8}$$

where

$$k_1 = \frac{(R_0 - R_1)\tan\beta}{R_0 \sin\alpha_0} = \frac{t \sec\beta \tan\beta}{R_0 \sin\alpha_0} \tag{9}$$

$$k_2 = \frac{-(R_0 - R_1)^2}{2R_0 \sin\alpha_0} = \frac{-t^2 \sec^2\beta}{2R_0 \sin\alpha_0} \tag{10}$$

Equations (2, 4, 9, and 10) have also been given in Refs. 4 and 5.

Since k_1 and k_2 are consants, the total spiral length is a linear function of z. The angle γ is called the tilt angle, which is defined as the angle between the local tangent to a constant θ curve and the z axis. Both of these lines lie in the vertical plane containing the constant θ curve (Fig. 2). The tilt angle can be determined by the total differentiation of the $\theta - \alpha$ Eq. (5) along a constant-θ curve, and using Eqs. (6) and (4). In doing so, we find that

$$\gamma(r,z) = \tan^{-1}\frac{dr}{dz} = \tan^{-1}\left[\frac{r\sqrt{z^2\tan^2\beta - R_0^2\sin^2\alpha_0}}{z\sqrt{r^2 - R_0^2\sin^2\alpha_0}}\right] \tag{11}$$

Equations (1-11) indicate that when R_0, R_1, R_2, α_0, and β are given, the entire warped surface is defined. The exact locations of all the points on the surface can now be determined as follows:

First, the bottom spiral BC ($z = z_B$) is divided into N_l equal segments of length ΔL_B. Substituting these individual arc lengths ($i \times \Delta L_B$, $i = 1,2,3,\ldots, N_l$) into Eqs. (7) and (4), one can solve for the corresponding radial distances r_i and the arc angles α_i. Then the value of θ_i can be determined from Eq. (5) with $\theta_0 = 0$. Thus, the exact (r,θ,z) locations of all the points along BC have been established. For points on any other spiral ($z \neq z_B$), the same procedure can be taken to determine their exact coordinates. However, in order to determine points located on the ($N_l + 1$) constant θ lines associated with the bottom spiral BC (Fig. 3), Eq. (5) is transposed as

$$\alpha + \cot\alpha = \bar{\alpha} + \cot\bar{\alpha} - \theta \tag{12}$$

where θ is known from the bottom spiral BC. For a given z, the value of α is defined by Eq. (6) and $\bar{\alpha}$ is determined by Newton's method[3] with an extremely rapid convergence rate. Hence, the radial coordinate r can be readily determined by Eq. (4). Proceeding with this scheme from the bottom to the top with a step size $\Delta z = h/N_h$, one can establish the exact coordinates of all the ($N_h + 1$) points along the corresponding constant-θ curve. While the exact coordinates of points on the generator AB are obtained by plane geometry as ($z \tan\beta$, 0, z), the exact chord length between any two points, such as A and E, E and F (Fig. 3), etc., can be directly computed by

$$d = \left[(r_2\cos\theta_2 - r_1\cos\theta_1)^2 + (r_2\sin\theta_2 - r_1\sin\theta_1)^2 + (z_2 - z_1)^2\right]^{1/2} \tag{13}$$

where subscripts 1 and 2 define the points of interest.

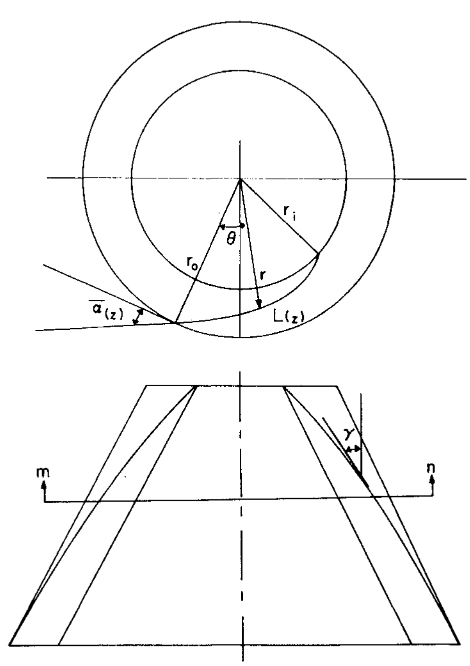

Fig. 2 Typical cross section.

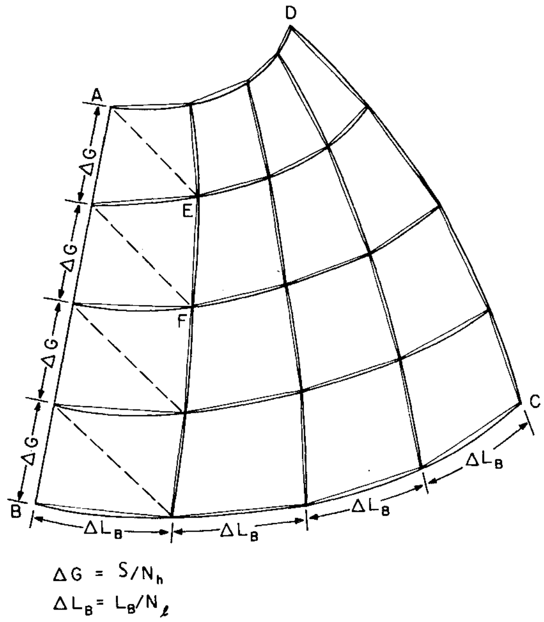

Fig. 3 Exact warped surface.

Approximate Development

As mentioned earlier, the exact warped surface cannot be developed from a flat sheet. This is not surprising since warped surfaces are "those which may be generated by moving a straight line so that any two consecutive positions of the generating line are skew lines."[2] Consequently, it is necessary to adopt an approximate procedure. While classical approximate development approaches are available,[2] they depend upon discontinuous sheet patterns in the present case, i.e., cuts are required in the basic sheet pattern. Therefore, these methods are not considered acceptable. An alternate approach involves interconnection of a finite number of points on the surface to form a figure defined by a large number of triangular elements. As the elements shrink in size, this figure approaches the desired surface in the limit. While this figure can be developed exactly, the associated basic sheet pattern is again discontinuous. Another alternative involves derivation of a new sheet pattern, i.e., abandoning that given by Eq. (4). However, this approach destroys the axisymmetric feature and the continuity property of the geometry dictated by Eq. (4). Hence, it will be necessary to present a new approach to define an approximate development procedure for the warped basic sheet pattern. In this procedure, the lengths of line segments on the perimeter of the warped sheet are preserved in the limit.

The procedure begins by dividing the bottom spiral into N_l equally spaced points, as suggested by the intersection of the constant-θ and constant-z trajectories. For fairly small values of N_l, however, the region adjacent to the right-hand border may be inadequately described in this approach. Therefore, a "boundary-layer" region is introduced here to avoid this lack of definition. This simply involves the use of additional constant-θ lines, those which originate at the intersection of the various z lines with the right-hand boundary. Next follows the computation of the true chord lengths joining the neighboring grid points. These are given by Eq. (13). At this time, the approximate process begins. As shown in Fig. 4, points 1 and 2 are first placed on the y axis at a distance ΔG apart, where $\Delta G = S/N_h$. Point 1′ is then determined by the intersection of chords d_1 and d_2. This involves selecting the appropriate root from the solution of the simultaneous albegraic equations:

$$(x-x_1)^2+(y-y_1)^2=d_1^2$$
$$(x-x_2)^2+(y-y_2)^2=d_2^2 \qquad (14)$$

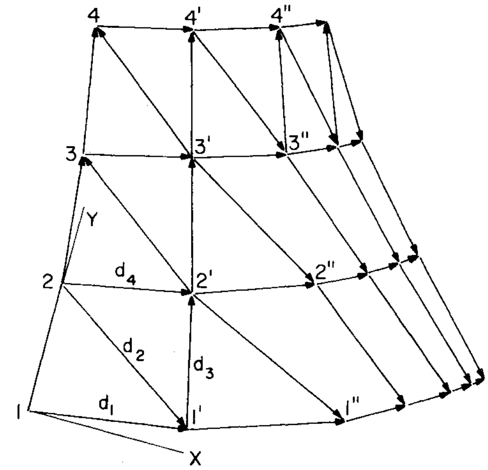

Fig. 4 Approximate development.

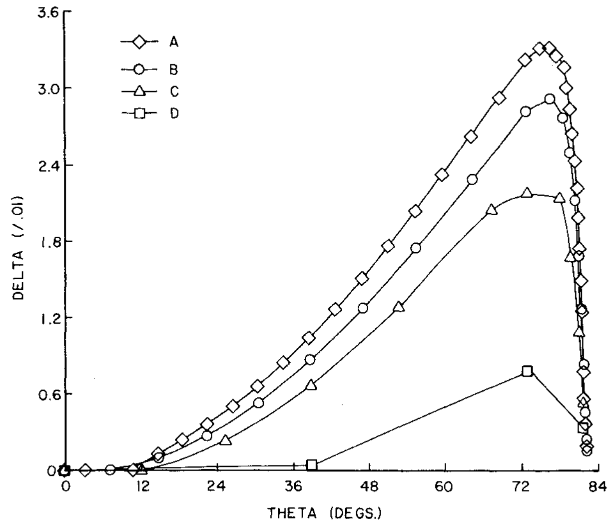

Fig. 5 Stretching displacement.

where (x_1, y_1) and (x_2, y_2) are the coordinates of the two known points. Likewise, point 2′ can be determined by two chord lengths d_3 and d_4, followed by points 3, 3′, 4, 4′, etc., until all the points on the first two θ curves are mapped on this xy plane. For points corresponding to the remaining constant-θ curves, such as 1′, 2′, 3′, etc., the same procedure has been taken, except that the true length requirement must be abandoned between 1″ and 2″, 2″ and 3″, i.e., between those points not connected in Fig. 4. This observation stems from consideration of the three-dimensional geometry of the triangular planes surrounding a point such as 2′, 3′, or 3″. Since these planes are, in general, distinct, the sum of the adjacent dihedral angles differs from 360 deg. This precludes a planar construction in which all triangles surrounding a given point are represented in true size. This is also an indication of the approximate nature of the present approach. The arrows represent true chords of the approximation process. It is also noted that the points on the right-hand boundary corresponding to the inner cone are located on different θ lines. This is to be expected since the radial coordinates and the associated angles for these boundary points are

$$r_{\text{end}} = z\tan\beta - (R_0 - R_I) \qquad (15)$$

and

$$\alpha_{\text{end}} = \sin^{-1}\left[\frac{z\tan\beta - (R_0 - R_I)}{R_0 \sin\alpha_0}\right] \qquad (16)$$

respectively. Therefore, via Eq. (5), θ end depends on z.

One might expect the occurrence of numerical instabilities as the values of N_h and N_l become large. Such a problem, however, has not been encountered thus far with both the single- and double-precision options on the CDC 6600 system. In the event they do occur, a simple remedy involves omitting a number of θ lines at a time along the right-hand boundary line. This procedure may also be applied to obtain a grid system with a more uniform appearance.

Error Assessment

In the previous section, an approach was considered to perform an approximate development of the basic sheet element of a rosette cone. Here, a scheme is presented to define the quality of the approximation; i.e., to establish the credibility of the approximate development procedure. Conceptually, the scheme involves the assumption that the basic sheet may be modeled as a membrane, which is then stretched until the node points coincide with their counterparts on the exact surface. If the local values of the unit stretch are sufficiently small, the approximation is a good one. While it cannot be proven that the approach is universally valid, it can be shown, for configurations using exaggerated values of the input parameters (those which tend to magnify the errors and are greater than those used in practice), that the unit stretch distributions are quite small.

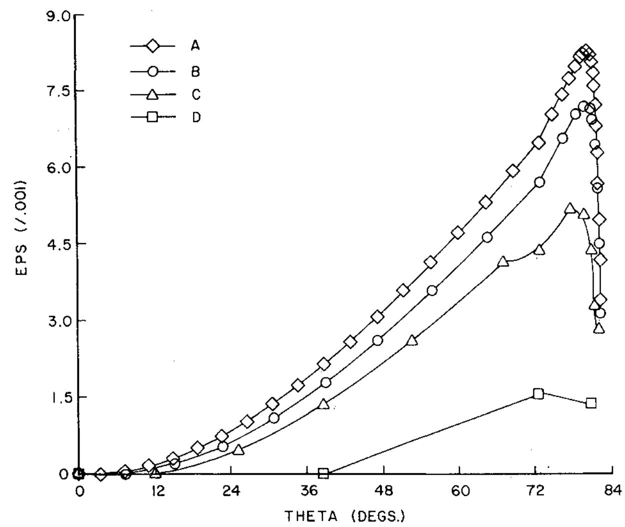

Fig. 6 Unit stretch (strain).

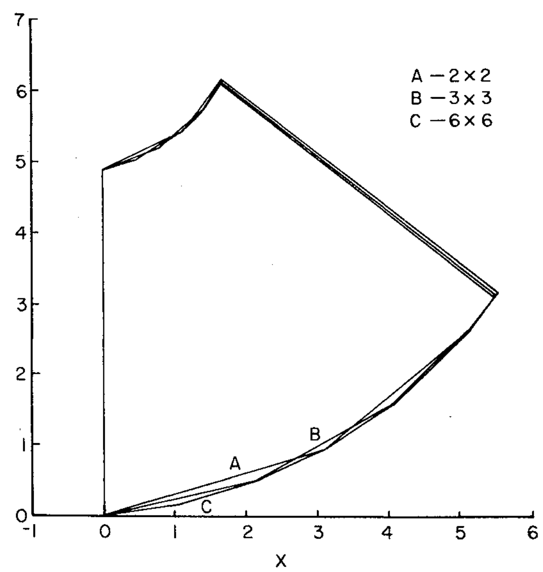

Fig. 7 Basic sheet pattern vs $N_h = N_l$.

Recall that true lengths of all the horizontal chords (Fig. 4) were employed throughout the approximate scheme. Clearly, as the value of N_l becomes large, the lengths of these chords will approach the corresponding segments of the spiral length. Hence, the unit stretch along the spirals approaches zero with an increase in N_l.

The unit stretch along the constant-θ lines, on the other hand, does not behave the same way. This can be observed from Figs. 5 and 6 (see Appendix for input data), where curves A, B, C, D, corresponding to $N_h \times N_l = 20 \times 20$, 10×10, 6×6, and 2×2, respectively, indicate that the errors are small. The Δ (or DELTA) of Fig. 5 represents the difference between the constant-θ curve length and the respective length in the basic sheet pattern. The ϵ (or EPS) of Fig. 6 is defined to be the ratio of Δ to the θ curve length. Note that all unit stretch values are several orders of magnitude smaller than unity, so that, for the given configuration, the approach is quite accurate. While it may appear the lower values of N_h and N_l lead to a better approximation, as indicated by Figs. 5 and 6, this is not necessarily true, since only the error due to stretching has been evaluated. Another measure of error exists; namely, the distance between a point on a node-connecting chord and its associated point on the exact surface, i.e., a measure of deflection. This deflection error, although quite large for small vaues of N_h, approaches zero as N_h becomes larger. Hence, the total error involves a combination of two effects; that is, the use of unit stretch alone is not a valid criterion for defining N_h and N_l to minimize the error in the approximate development. It is suggested, without proof, that larger values of N_h and N_l be used in practice. As these values approach infinity, examples have shown that a limiting, unique pattern is approached. For example, see Fig. 7 where patterns of 2×2, 3×3, and 6×6 are displayed as A, B, C, and Fig. 8, where the maximum unit stretch becomes asymptotic for large values of N.

Concluding Remarks

A geometrical analysis of the Rosette® cone and an approximate approach to develop the basic sheet pattern have been presented. The basic analysis was based upon the rosette cylinder analysis of Ref. 1, where each horizontal cross

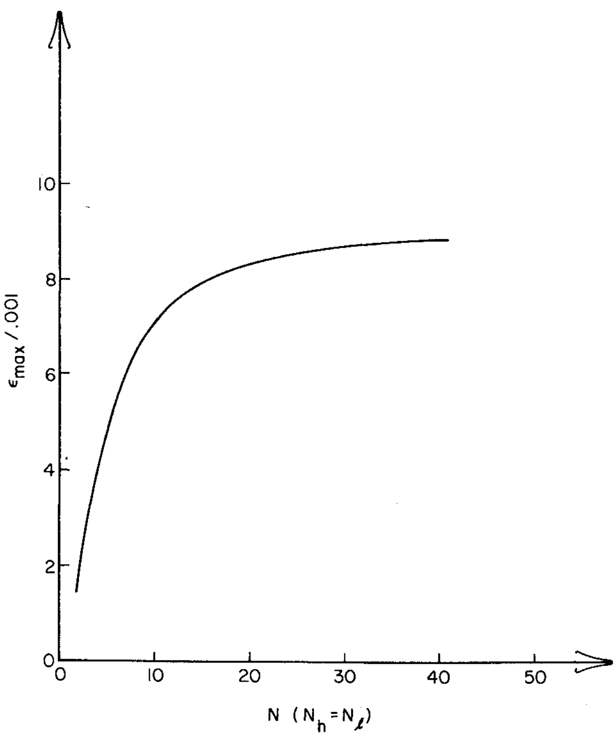

Fig. 8 Maximum unit stretch vs N.

section of the warped basic sheet follows a certain spiral trajectory dictated by Eqs. (5) and (6). While this warped surface is not developable from a flat sheet, results of the approximate approach indicated that the errors associated with the approximation are small for practical configurations. The concept of unit stretching was then introduced to deform the flat sheet unitl the node points coincide with their counterparts on the exact surface. From the resulting errors, it is concluded that the amount of stretching needed is small and the approximate scheme will be quite applicable in the actual fabrication of the rosette cone.

Appendix

Variable Wall Thickness

Consider a body in which the inner surface is that of a right circular cone and the outer surface is an arbitrary body of revolution. In this case, the warped sheet coincides with a generator along the inner surface. The relation

$$R_1 \sin\alpha_1 = R_0 \sin\alpha_0 \tag{A1}$$

defines the value α_1, which is the starting value of α in this case. Equation (A1) is employed to incorporate the appropriate parameters into Eqs. (2, 4, 5, and 6). Equations (8-10) are no longer valid, of course, since they were specifically developed for the case of constant wall thickness.

Sample Input Data

The sample problem consists of the following input data:

$$\begin{aligned} \alpha_0 &= 20 \text{ deg} \\ R_0 &= 2 \text{ units} \\ R_1 &= 1 \text{ unit} \\ R_2 &= 4 \text{ units} \\ \beta &= \sin^{-1}[8/13] \\ h &= 4.875 \cos\beta \text{ units} \end{aligned} \tag{A2}$$

Acknowledgments

The authors wish to express their appreciation to S.W. Tsai for his suggestions and discussion, to the UDRI Graphic Arts Section for preparing figures and vu-graphs, and to B. Drake and P. Thomas for typing the manuscript. They also wish to acknowledge the software assistance by J.S. Solomon, G. Fultz, D. Summers, and D. Walters.

References

[1] Pagano, N.J., "Elastic Response of Rosette Cylinders under Axisymmetric Loadings," *AIAA Journal,* Vol. 15, Feb. 1977, pp. 159-166.

[2] Wellman, B.L., *Technical Descriptive Geometry,* McGraw-Hill Book Co., New York, 1948.

[3] Conte, S.D. and deBoor, C., *Elementary Numerical Analysis,* McGraw-Hill Book Co., New York, 1972.

[4] Abildskou, D.P.A., "Rosette Analysis," Hitco Stress Rept. AD-66-1, 1966.

[5] Zak, A., "Rosette Flat Pattern Analysis," Hitco Stress Rept. AD-66-4, 1966.